Electromagnetic propulsion and separation by chirality of nanoparticles in liquids

E. Kirkinis, A. V. Andreev, and B. Spivak

Phys. Rev. E **85**, 016321 — Published 25 January 2012

DOI: 10.1103/PhysRevE.85.016321

Electromagnetic propulsion and separation by chirality of nanoparticles in liquids

E. Kirkinis*

University of Washington, Department of Applied Mathematics, Seattle WA 98195

A.V. Andreev and B. Spivak

University of Washington, Department of Physics, Seattle, WA 98195

Abstract

We introduce a new mechanism for the propulsion and separation by chirality of small ferromagnetic particles suspended in a liquid. Under the action of a uniform d.c. magnetic field **H** and an a.c. electric field **E** isomers with opposite chirality move in opposite directions. Such a mechanism could have a significant impact on a wide range of emerging technologies. The component of the chiral velocity that is odd in **H** is found to be proportional to the intrinsic orbital and spin angular momentum of the magnetized electrons. This effect arises because a ferromagnetic particle responds to the applied torque as a small gyroscope.

PACS numbers: 47.63.mf, 87.80.Ek, 87.50.ch

*Electronic address: kirkinis@amath.washington.edu

I. INTRODUCTION

Recent years have witnessed an explosion of interest in the fabrication of nanoscale objects [1–4] and their propulsion in liquids mostly due to their application to emerging technologies [5]. Numerous mechanisms have been proposed to achieve this propulsion ranging from electrophoresis for platinum rods [6], to beating of flexible magnetic rods resembling flagella [7]. Some mechanisms take advantage of the lack of center-symmetry *in the shape* of the particles and propel them under the action of rotating external fields [1, 8, 9].

In this article we introduce a new mechanism for the propulsion and separation by shape chirality of small ferromagnetic isomers suspended in a liquid. The separation by chirality is induced by applying a uniform linearly polarized a.c. electric field $\mathbf{E}(t) = \mathbf{E}\sin(2\pi\nu t)$ and a d.c. magnetic field $\mathbf{H}$. We consider a generic situation in which the particles do not possess any special symmetries. Because of the anisotropy of the workfunction [10] such particles must have a nonzero electric dipole moment $\mathbf{d}$, whose magnitude may be estimated as eR [12]. We emphasize that $d \neq 0$ does not imply ferroelectricity, which would result in $d \propto R^3$, where R is the particle size. Electric dipole moments of non-ferroelectric nanoparticles have been recently measured [11]. We note that in a given particle the direction of the electric dipole moment $\mathbf{d}$ is unique. In contrast, the magnetic moment $\mathbf{M}$ can acquire different orientations with respect to the crystalline axes. Here we consider particles with an easy axis magnetic anisotropy. In a suspension of such particles the two possible magnetization values, $\mathbf{M}$ and $-\mathbf{M}$, are realized with equal probabilities. We consider the general case where $\mathbf{d}$ and $\mathbf{M}$ are non collinear, and so are $\mathbf{E}$ and $\mathbf{H}$. In what follows, we will be interested in the time-averaged chiral velocity $\mathbf{V}_{ch} = V_{\circlearrowright} - V_{\circlearrowleft}$ in a racemic suspension of such particles. Here $V_{\circlearrowright}$ and $V_{\circlearrowleft}$ are the velocities of the right and left-handed particles, respectively.

The direction of the $\mathbf{V}_{ch}$ is defined by the external fields. Due to the oscillatory character of the electric field it must remain unchanged under $\mathbf{E} \to -\mathbf{E}$. Since $\mathbf{H}$ is an axial vector and $\mathbf{E}$ a polar vector, the most general expression for $\mathbf{V}_{ch}$ allowed by symmetry can be written in the form

$$\mathbf{V}_{ch} = \sigma_1 \mathbf{h} + \sigma_2 (\mathbf{e}\cdot\mathbf{h})\,\mathbf{e} + \sigma_3 (\mathbf{e}\cdot\mathbf{h})[\mathbf{e}\times\mathbf{h}]. \tag{1}$$

Here $\mathbf{h}$ and $\mathbf{e}$ are unit vectors in the direction of the magnetic and electric fields respectively. The phenomenologically introduced coefficients σ_i depend on the particle shape, frequency ν, field strengths, temperature etc. and have opposite signs for isomers of opposite chirality.

Thus, particles of opposite chirality will move in opposite directions.

It is important to note that a ferromagnetic particle possesses an intrinsic angular momentum associated with the magnetized electrons, $\mathbf{L}_e = \mathbf{M}/\gamma$ [13]. The gyromagnetic ratio γ can be estimated as $\gamma \sim e/mc$, where m and e are the electron mass and charge, and c is the speed of light. The value of $\mathbf{L}_e$ is relatively small, and it is usually neglected in studies of the dynamics of small ferromagnetic particles. However the existence of $\mathbf{L}_e \neq \mathbf{0}$ means that the particle responds to external torques as a small gyroscope. This leads to new physical effects.

We show below that the coefficients σ_1 and σ_2 in Eq. (1), which describe chiral separation in the **E**-**H** plane, are proportional to $L_e \equiv |\mathbf{L}_e|$. On the other hand, the coefficient σ_3 in the third term, describing chiral separation perpendicular to the **E**-**H** plane, remains finite even as $L_e \to 0$. The vanishing of σ_1, σ_2 at $L_e = 0$ can be seen from the following consideration. In the approximation where $L_e = 0$ the magnetic moment affects the particle motion only via the external torque

$$\boldsymbol{\tau} = \mathbf{M} \times \mathbf{H} + \mathbf{d} \times \mathbf{E}(t). \tag{2}$$

Thus, in this approximation all terms in the velocity of a particle that are odd in **H** should also be odd with respect to **M**. Consequently, these terms vanish upon averaging over different realizations of **M**. On the other hand, since $\mathbf{L}_e \propto \mathbf{M}$ the chiral current can contain terms which are odd in **M** and linear in $\mathbf{L}_e$, which do not vanish upon averaging over different realizations of the particle magnetization **M**.

II. CHIRAL SEPARATION IN THE CREEPING-FLOW REGIME

The motion of small particles in a dilute suspension can be described using the formalism of low Reynolds number hydrodynamics, in which the external forces, $\boldsymbol{F}$, and torques, $\boldsymbol{\tau}$, are linearly related to the instantaneous linear and angular velocities, $\mathbf{v}$ and $\boldsymbol{\omega}$, by a resistance matrix [14]

$$\begin{pmatrix} \boldsymbol{F} \\ \boldsymbol{\tau} \end{pmatrix} = \eta \begin{pmatrix} \hat{K} & \hat{C} \\ \hat{C} & \hat{\Omega} \end{pmatrix} \begin{pmatrix} \mathbf{v} \\ \boldsymbol{\omega} \end{pmatrix} + \begin{pmatrix} 0 \\ \boldsymbol{\omega} \times \mathbf{L}_e \end{pmatrix}. \tag{3}$$

Here η is the liquid viscosity. For a particle of characteristic size R the translation $\hat{K} \sim R$, coupling $\hat{C} \sim R^2$ and rotation $\hat{\Omega} \sim R^3$ matrices depend only on the particle's geometry. The coupling matrix $\hat{C}$ relates pseudo-vectors $\boldsymbol{\omega}$ and τ to polar vectors **F** and $\mathbf{v}$. Therefore it

vanishes for non-chiral particles. Above, we have tacitly assumed that the resistance matrix is expressed with respect to a unique fixed point on the particle called the reaction center which requires that $\hat{C}$ is symmetric. The third term in Eq. (3) describes the gyroscopic effect.

We assume that the particles are uncharged so that the electric field does not exert a force on them, $\boldsymbol{F} = \mathbf{0}$. In this case Eq. (3) gives a linear relation between the propulsion velocity $\mathbf{v}$ and $\boldsymbol{\omega}$

$$\mathbf{v} = -\hat{K}^{-1}\hat{C}\boldsymbol{\omega}. \tag{4}$$

This relation expresses the so-called propeller effect. Rotation of chiral particles caused by the external torques is accompanied by translational motion. Since the coupling matrix $\hat{C}$ has opposite sign for particles with opposite chirality [14] (while $\hat{K}$ and $\hat{\Omega}$ remain the same), it is clear that particles of opposite chirality subjected to the same torque will move in opposite directions.

To describe the rotation of the particle we use body and laboratory axes defined by the unit vectors $\hat{\mathbf{x}}_1, \hat{\mathbf{x}}_2, \hat{\mathbf{x}}_3$, and $\hat{\mathbf{x}}, \hat{\mathbf{y}}, \hat{\mathbf{z}}$ respectively whose relative orientation is specified by the three Euler angles ϕ, θ and ψ [15]. Using this notation, the balance of angular momentum (3) determines the evolution equation of the Euler angles

$$\begin{pmatrix} \dot{\phi} \\ \dot{\theta} \\ \dot{\psi} \end{pmatrix} = \hat{Q}\widetilde{\Omega}_e^{-1} \begin{pmatrix} \tau_{x_1} \\ \tau_{x_2} \\ \tau_{x_3} \end{pmatrix}. \tag{5}$$

where $\hat{Q}$ is the matrix connecting the particle angular velocity with the derivatives of the Euler angles. Its representation in, for example, the body frame is

$$\hat{Q} = \frac{1}{\sin\theta} \begin{pmatrix} \sin\psi & \cos\psi & 0 \\ \sin\theta\cos\psi & -\sin\theta\sin\psi & 0 \\ -\cos\theta\sin\psi & -\cos\theta\cos\psi & \sin\theta \end{pmatrix} \tag{6}$$

(see [15]). The rotational resistance matrix $\widetilde{\Omega} = \eta(\hat{\Omega} - \hat{C}\hat{K}^{-1}\hat{C})$ is augmented

$$(\widetilde{\Omega}_e)_{ij} = (\widetilde{\Omega})_{ij} + \varepsilon_{ijk}(\mathbf{L}_e)_k, \tag{7}$$

to account for the presence of the intrinsic angular momentum $\mathbf{L}_e$.

In general the torques and forces in Eq. (3) consist of the deterministic torques of Eq. (2) and random torques and forces arising from thermal fluctuations. In this case the

system can be described by the Fokker-Planck equation for the particle distribution function $f = f(t, \mathbf{o})$ [16]

$$\left(\frac{\partial}{\partial t} - \boldsymbol{\mathcal{R}} kT \widetilde{\Omega}_e^{-1} \boldsymbol{\mathcal{R}}\right) f = \boldsymbol{\mathcal{R}} \widetilde{\Omega}_e^{-1} f \boldsymbol{\mathcal{R}} U, \tag{8}$$

and the following expression for the ensemble averaged chiral velocity

$$\mathbf{V}_{ch} = \nu \int_0^{1/\nu} dt \int d^3\mathbf{o}\, \hat{b}\, (kT \boldsymbol{\mathcal{R}} f + f \boldsymbol{\mathcal{R}} U)\,. \tag{9}$$

Here T is the temperature, k is the Boltzmann constant, $U = -\mathbf{d}\cdot\mathbf{E} - \mathbf{M}\cdot\mathbf{H}$, $\hat{b} = -\frac{1}{\eta}\hat{\Omega}^{-1}\hat{C}(\hat{K} - \hat{C}\hat{\Omega}^{-1}\hat{C})^{-1}\widetilde{\Omega}\widetilde{\Omega}_e^{-1}$, $\mathbf{o}$ denotes the particle orientation (specified by the Euler angles), and we have tacitly assumed that the magnetic and electric dipole moments due to polarization of the particle are small compared to the permanent ones. The tensor and vector quantities in the integrand must be evaluated in the laboratory frame and are time-dependent because of the changing orientation of the particle. The operator $\boldsymbol{\mathcal{R}}$ is a gradient in the space of rotations [13, 17] ($-i\boldsymbol{\mathcal{R}}$ is the quantum mechanical angular momentum). Choosing, for example, body frame coordinates, $\boldsymbol{\mathcal{R}}$ can be represented in the form

$$\begin{pmatrix} \mathcal{R}_{x_1} \\ \mathcal{R}_{x_2} \\ \mathcal{R}_{x_3} \end{pmatrix} = \begin{pmatrix} \frac{\sin\psi}{\sin\theta} & \cos\psi & -\cot\theta\sin\psi \\ \frac{\cos\psi}{\sin\theta} & -\sin\psi & -\cot\theta\cos\psi \\ 0 & 0 & 1 \end{pmatrix} \begin{pmatrix} \frac{\partial}{\partial\phi} \\ \frac{\partial}{\partial\theta} \\ \frac{\partial}{\partial\psi} \end{pmatrix}.$$

These equations describe diffusion in the particle orientation space and the translational motion associated with its rotation relative to the liquid (we assume that the spatial distribution of particles is uniform).

The strength of thermal fluctuations is characterized by the dimensionless parameters MH/kT, and dE/kT. We consider an electric field of frequency ν, $\mathbf{E}(t) = \mathbf{E}\sin(2\pi\nu t)$. In this case another important parameter is the ratio of the frequency ν to the rotational equilibration rate, $\nu\eta R^3/kT$.

For $MH/kT, dE/kT \ll 1$ Eqs. (8-9) can be solved by perturbation theory. At low frequencies, $\nu\eta R^3/kT \ll 1$, we obtain

$$\sigma_1 \sim \sigma_2 \sim \chi R\nu \frac{L_e\nu}{kT}\left(\frac{dE}{kT}\right)^2 \frac{MH}{kT}, \tag{10}$$

where $\chi \sim K^{-1}C/R$ is a dimensionless measure of the particle chirality. Because of the oscillatory character of the electric field, a nonvanishing time-averaged chiral velocity arises

starting from the first order in MH and second order in dE. Note that σ_3 arises only at fourth order in the perturbation theory, leading to the estimate $\sigma_3 \sim \chi\nu R\nu\eta R^3(dEMH)^2/(kT)^5$.

In the opposite regime, $MH/kT, dE/kT, \nu\eta R^3/kT \gg 1$, thermal fluctuations may be neglected and the motion of particles is described by the deterministic equations (2), (3) and (4). In this case, under the influence of **E** and **H** the particle orientation changes periodically with time and traces a cycle in the space of orientations. Relation (4) shows that propulsion is possible only if this cycle is non-self-retracing. This is the analogue of the "clam shell" theorem [18] for forced propulsion at low Reynolds numbers. It is worth noting that although the cycle traced by the linearly polarized electric field is self retracing, the cycle traced by body orientations is not.

At low frequencies where $\nu \ll \frac{dE}{\eta R^3}$ and $\nu \ll (MH)^2/(dE\eta R^3)$, the frequency dependence of the propulsion velocity is linear

$$\sigma_{1,2} \sim \chi\nu R(L_e/\eta R^3), \tag{11}$$

in contrast to the quadratic dependence in the strong fluctuation regime (10). The σ_3 component of velocity has a superlinear dependence on the frequency, see Eq. (13) below. Therefore at low frequencies the propulsion velocity is confined to the **E**-**H** plane.

The linear frequency dependence of the propulsion velocity is a feature which often arises in the adiabatic regime, where the orientation of the particle corresponds to instantaneous equilibrium. This occurs, for example, in the case where the electric field **E** is circularly polarized [1, 9].

For a linearly polarized electric field and constant magnetic field, the origin of the linear dependence on ν in Eq. (11) is more subtle. In this case the adiabatic approximation holds during most of the oscillation period. During these intervals the particle orientation is determined by the instantaneous values of $\mathbf{E}(t)$ and **H**, and the trajectory of the particle is self-retracing. However, the adiabatic approximation is violated at time intervals where $\mathbf{E}(t)$ is approximately zero. During these times the equilibrium orientation of the particle is not unique: the particle can rotate freely about the axis pointing along **M**, which is aligned with **H**. Most of the particle's rotation and propulsion occurs near these instances. As the electric field changes sign the particle rotates about **M** by an angle π. The direction of rotation is determined by corrections to the adiabatic approximation, which break the symmetry between clockwise and anticlockwise rotations, and lead to a non-self retracing

cycle and non-vanishing propulsion velocity linear in ν. However, if $\mathbf{L}_e = 0$, upon reversal $\mathbf{M} \to -\mathbf{M}$, the direction of the rotation and propulsion velocity also reverses. Therefore $\mathbf{V}_{ch}$ averaged over realizations of $\mathbf{M}$ vanishes. Accounting for the finite value of L_e results in the difference of the resistance tensors $\widetilde{\Omega}_e$ in states with $\pm\mathbf{M}$, and incomplete cancellation of contributions to $\mathbf{V}_{ch}$ from particles with different values of $\mathbf{M}$. This leads to Eq. (11).

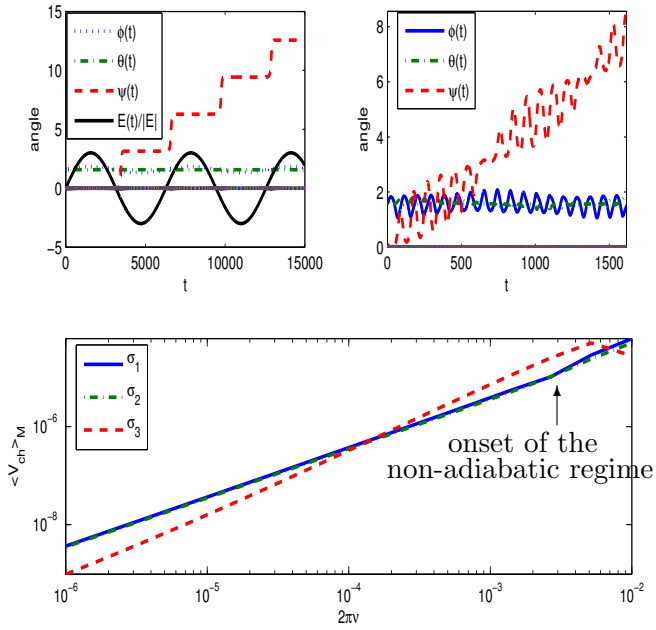

FIG. 1: (color online) Upper left: time dependence of the electric field and the Euler angles at low frequencies. The angle ψ increases in a stepwise fashion. Upper right: breakdown of the staircase at higher frequencies. Lower: log log plot of the averaged-over-M chiral velocity versus frequency. The frequency exponent of σ_1 and σ_2 (overlapping straight lines) is 1 at low frequencies and that of σ_3 is (approximately) 5/4 as discussed above Eq. (13). For higher frequencies the motion enters a non-adiabatic regime which changes the values of the aforementioned exponents, a fact reflected by cusp-like features in the frequency dependence of the propulsion velocity. Eq. (12) shows an example of the resistance tensor used in the simulation ([14] sec. 5.4).

Numerical solutions of the equations of motion, Eq. (3) confirm this picture. We choose $\hat{x}_3 \parallel \mathbf{M}$, so that the Euler angle $\psi(t)$ corresponds to rotation of the particle about $\mathbf{M}$. Typical results of numerical solutions of Eq. (3) are presented in Figures 1 and 2. The

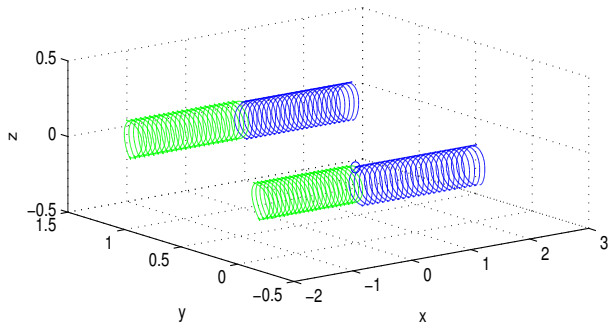

FIG. 2: (color online) Particle trajectories in the laboratory frame for mutually perpendicular **H** and **E** directed along the x and y axes respectively. In this case last two terms in Eq. (1) vanish and chiral separation occurs only along the **H** direction. The motion of particles with opposite values of **M** are shown in blue and green. The trajectories originate from the same point and move on average in the positive (blue) and negative (green) x-direction. The trajectories in the background are calculated with $L_e = 0$. In this case the displacements for opposite **M** are opposite and the chiral velocity averaged over realizations of **M** vanishes. The trajectories in the foreground are computed with $L_e \neq 0$. In this case the magnitudes of displacements for opposite values of **M** are different and averaging over **M** leads to a finite chiral velocity. Eq. (12) shows an example of the resistance tensor used in the simulation ([14] sec. 5.4).

resistance matrix used therein acquires, in principal axes, the representation ([14] sec. 5.4)

$$\begin{aligned}
\hat{K} &= \frac{32}{3} c \,\mathrm{diag}[2+\cos^2(\zeta), 2+\sin^2(\zeta), 2], \\
\hat{C} &= \frac{32}{3} ch \sin(\zeta)\cos(\zeta)\,\mathrm{diag}[1,-1,0], \\
\hat{\Omega} &= \frac{32}{3}\,\mathrm{diag}[ch^2(2+\sin^2(\zeta)+2\frac{c^2}{h^2}), \\
&\qquad ch^2(2+\cos^2(\zeta)+2\frac{c^2}{h^2}), 2c^3].
\end{aligned} \tag{12}$$

The above resistance matrix corresponds to a two-blade propeler-like particle formed by joining to the ends of a thin rod two circular discs of radius c with center to center spacing $2h$. The smaller angle between the planes of the disks is here denoted by ζ.

The time evolution of the angle ψ exhibits a staircase structure, increasing (on average) linearly with t (see the upper panels in Fig.1). At low frequencies there are two steps per oscillation period and each step corresponds to a rotation of the particle about **M** by an

angle π, as in the upper left of Fig.1. In this regime the σ_1 and σ_2 components of the propulsion velocity are linear with respect to the frequency ν, whereas the σ_3 component scales as $\nu^{1+\alpha}$ with $\alpha \approx 0.25$, as shown in the lower panel in Fig.1. In the absence of thermal noise σ_3 can be expressed as $\sigma_3 \sim \chi\nu R f\left(Ed/MH, \nu\eta R^3/MH\right)$, where $\chi\nu R$ is the characteristic scale for the chiral velocity in the adiabatic regime, and $f(x,y)$ is an unknown function that describes deviations from adiabaticity and depends on the only dimensionless parameters in the problem, dE/MH and $\nu\eta R^3/MH$. Most of the propulsion occurs near the instances $t_n = n/\nu$, where the electric field changes sign and depends linearly on time, $E(t) \approx 2\pi\nu E(t - t_n)$. Thus we conclude that deviations from adiabaticity depend only on the product νE. In other words $f(x,y)$ depends only on the products xy. Combining this with the numerical observation of the power law frequency dependence we obtain the following estimate for σ_3 in the low frequency regime,

$$\sigma_3 \sim \chi\nu R \left[\frac{\nu\eta R^3 dE}{(MH)^2}\right]^{\alpha}. \tag{13}$$

As the frequency ν increases, the character of the motion undergoes a series of bifurcations: the step-like character of evolution of $\psi(t)$ is preserved but the steps become separated by several oscillation periods (see the upper right panel in Fig.1). This leads to cusp-like features in the frequency dependence of the propulsion velocity (see the lower panel in Fig. 1).

When $L_e = 0$, particles with opposite values of $\mathbf{M}$ rotate and move in opposite directions in the $\mathbf{H}$-$\mathbf{E}$ plane, leading to a vanishing planar displacement upon averaging over the directions of $\mathbf{M}$. In contrast, when $L_e \neq 0$ the in-plane displacement averaged over $\mathbf{M}$ is finite. This is illustrated in Fig. 2 for the case when $\mathbf{H}$ and $\mathbf{E}$ are perpendicular to each other.

We now estimate the magnitude of the above effect. Assuming that a single domain ferromagnetic particle is roughly spherical, we get an estimate for the dimensionless parameter characterizing the magnitude of the gyroscope effect,

$$\frac{L_e}{\widetilde{\Omega}} \sim \frac{s\hbar n}{6\eta}, \tag{14}$$

independent of the particle size. Here n is the volume density of magnetic atoms, $\hbar$ is Planck's constant, and s is the spin per atom (in units of $\hbar$), which in different materials can lie in the range $1 - 10^{-2}$. Using the viscosity of water at normal conditions, $\eta \sim 10^{-2}$g/cm·s, and $n \sim 10^{23}$cm^{-3} we get $L_e/\widetilde{\Omega} \sim (s/6) \times 10^{-2}$. The estimate Eq. (11) holds

provided the inequalities $\nu < dE/(\eta R^3)$, $\nu < (MH)^2/(\eta R^3 dE)$ and $dE, MH > kT$ are satisfied. In modern experiments [19] electric fields in excess of 10^6 V/m at frequencies 1 MHz have been realized in aqueous solutions. Estimating $d \sim eR$ [11, 12] we see that the required inequalities are satisfied for a particle size $R \sim 100$ nm. The magnetic restriction, $MH/kT \gg 1$, is satisfied even in weak magnetic fields for a ferromagnetic particle of this size. Assuming that the degree of chirality is $\chi \sim 0.1$, $H \sim 10$ Gauss and $d \sim 10^4 D$ and using Eqs. (11) and (13) with the aforementioned electric fields and frequencies we get the estimates

$$\sigma_{1,2} \sim (0.1 - 10)\,\mu\text{m/s}, \quad \sigma_3 \sim 1\,\text{mm/s}, \tag{15}$$

which show that the effect is detectable.

Finally, we point out the existence of another class of effects that are generically related to the one discussed above. These are realized by replacing the linearly polarized a.c. electric field $\mathbf{E}$ with either a gradient of temperature ∇T, pressure ∇P, or an oscillating magnetic field $\tilde{\mathbf{H}} = \tilde{H}\tilde{\mathbf{h}}$, where $\tilde{H} = a\sin(2\pi\nu t)$. To describe these effects on the phenomenological level one should make the following changes in Eq. (1): $\mathbf{e} \to \nabla T$, $\mathbf{e} \to \nabla P$, and $\mathbf{e} \to \tilde{\mathbf{h}}$ respectively. Calculating the corresponding coefficients which are analogues of the $\sigma_{1,2,3}$ in Eq. (1) is beyond the scope of the present article.

Acknowledgments: We are grateful to E. Ivchenko for useful discussions. This work was supported by DOE grant DE-FG02-07ER46452 (EK and AVA) and NSF grant DMR-0704151 (BS).

---

[1] A. Ghosh and P. Fischer, *Nano Letters*, 9(6):2243–2245, 2009.

[2] D. Zerrouki *et al.*, *Nature*, 455:07237, 2008.

[3] L. Zhang *et al.*, *Appl. Phys. Lett.*, 94(6), 2009.

[4] M. S. Sakar *et al.*, *Appl. Phys. Lett.*, 96(4):043705, 2010.

[5] J.-H. Lee *et al.*, *Nature Med.*, 13(1):95, 2007. R. Weissleder and M. J. Pittet, *Nature*, 452(7187):580, 2008. R. Weissleder *Science*, 312(5777):1168, 2006. C. Alexiou *et al.*, *Jl of Magn.and Magn. Mat.*, 293(1):389, 2005.

[6] W.F. Paxton *et al.*, *Jl of the Am. Chem. Soc.*, 126(41):13424–13431, 2004.

[7] R. Dreyfus *et al.*, *Nature*, 437(7060):862–865, 2005.

[8] U.K. Cheang *et al.*, *Appl.Phys.Lett.* , 97(21):213704, 2010.

[9] N.B. Baranova and B.Y. Zeldovich, *Chem. Phys. Lett.*, 57(3):435–437, 1978.

[10] L. D. Landau and E. M. Lifshitz. *Electrodynamics of Continuous Media. Course of Theoretical Physics, Vol. 2.* Pergamon Press, Oxford, 1984

[11] M. Shim and P. Guyot-Sionnest, *Jl. Chem. Phys.*, 111:6955, 1999.

[12] A.V. Shytov and M. Pustilnik, *Phys. Rev. B*, 76:041401, 2007.

[13] L. D. Landau and E. M. Lifshitz. *Quantum mechanics: non-relativistic theory. Course of Theoretical Physics, Vol. 3.* Pergamon Press, Oxford, 1958

[14] J. Happel and H. Brenner. *Low Reynolds number hydrodynamics with special applications to particulate media.* Prentice-Hall Inc., Englewood Cliffs, N.J., 1965.

[15] L. D. Landau and E. M. Lifshitz. *Mechanics.* Course of Theoretical Physics, Vol. 1. Pergamon Press, Oxford, 1960.

[16] M. Makino and M. Doi, *Jl. Phys. Soc. Japan. (10)*, 73:2739–2745, 2004.

[17] L. D. Favro, *Phys. Rev. (2)*, 119:53–62, 1960.

[18] E. M. Purcell, *Am. Jl of Phys.*, 45(1):3–11, 1977.

[19] M. Washizu and O. Kurosawa *IEEE Trans. Industry Appl.*, 26(6):1165–1172, 1990.